Journal of Molecular Catalysis B: Enzymatic 122 (2015) 240–247

Contents lists available at ScienceDirect

Journal of Molecular Catalysis B: Enzymatic

journal homepage: www.elsevier.com/locate/molcatb

Resolution of α/β-amino acids by enantioselective penicillin G acylase from *Achromobacter* sp.

Michal Grulich[a,b,*], Jan Brezovský[c], Václav Štěpánek[a], Andrea Palyzová[a], Eva Kyslíková[a], Pavel Kyslík[a]

[a] *Laboratory of Enzyme Technology, Institute of Microbiology,v.v.i., Academy of Sciences of the Czech Republic, Vídeňská 1083, 142 20 Prague 4, Czech Republic*
[b] *Department of Biochemistry, Faculty of Sciences, Charles University, Hlavova 8, 128 40 Prague 2, Czech Republic*
[c] *Loschmidt Laboratories, Department of Experimental Biology and Research Centre for Toxic Compounds in the Environment RECETOX, Masaryk University, Kamenice 5/A13, 625 00 Brno, Czech Republic*

ARTICLE INFO

Article history:
Received 26 June 2015
Received in revised form 19 August 2015
Accepted 18 September 2015
Available online 25 September 2015

Keywords:
Penicillin G acylase
Enantioselectivity
Homologous model
Docking experiments
α/β-amino acid

ABSTRACT

Penicillin G acylases (PGAs) are enantioselective enzymes catalyzing a hydrolysis of stable amide bond in a broad spectrum of substrates. Among them, derivatives of α- and β-amino acids represent a class of compounds with high application potential. PGA^{Ec} from *Escherichia coli* and PGA^{A} from *Achromobacter* sp. CCM 4824 were used to catalyze enantioselective hydrolyses of seven selected *N*-phenylacetylated α/β-amino acid racemates. The PGA^{A} showed higher stereoselectivity for enantiomers of *N*-PhAc-β-homoleucine, *N*-PhAc-α-*tert*-leucine and *N*-PhAc-β-leucine. To study the mechanism of enantiodiscrimination on molecular level, we have constructed a homology model of PGA^{A} that was used in molecular docking experiments with the same substrates. *In-silico* experiments successfully reproduced the data from experimental enzymatic resolutions confirming validity of employed modeling protocol. We employed this protocol to evaluate enantiopreference of PGA^{A} towards seven new substrates with application potential. For five of them, high enantioselectivity of PGA^{A} was predicted.

1. Introduction

Penicillin G acylases (EC 3.5.1.11; PGA, penicillin amidohydrolase) are robust industrial catalysts routinely used for decades for biotransformation of penicillins and cephalosporins [1–4]. Their biocatalytic potential expanded tremendeously once PGAs were found to be enantioselective and promiscuous [5]. Syntheses of semisynthetic β-lactam antibiotics, peptide syntheses and resolutions of racemic mixtures *via* enantioselective acylation or hydrolysis of broad range of substrates (*e.g.*, amino acids, ketones, amino acid esters or amides, amino nitriles or amino alcohols) catalyzed by PGAs represent biocatalyses with high potential especially for pharmaceutical industry. The PGAs are heterodimers composed of α- and β-subunit and belong to the structural superfamily of N-terminal nucleophilic hydrolases (Ntn hydrolases). Recent resolutions of three-dimensional PGA crystal structures provided detailed insight into the active site of this enzyme and allowed better understanding of a catalytic mechanism. An active site of PGA^{Ec} consists of two regions [6]: 1. aminic subsite preferring hydrophilic groups including catalytic aa residues Ser1ß, and other essential amino acid residues Gln23ß, Ala69ß and Asn241ß and 2. acyl binding subsite which accepts hydrophobic groups [7] consisting of Met142α, Arg145α, Phe146α, Phe24ß, Thr32ß, Pro49ß, Val56ß, Trp154ß and Ile177ß. Catalytic mechanism of hydrolysis of penicillin G, synthesis of ß-lactam antibiotics or enantioselective resolution involves the nucleophilic attack of the O^{γ} hydroxyl group of Ser1ß on the carbonyl carbon of the amide bond [8,9]. As the consequence of the attack, a covalent intermediate of an acyl-enzyme complex *via* a tetrahedral transition state is formed. Asn241ß and Ala69ß form the "oxyanion hole" that balances the negative charge and thus lowers the energy of the reactive tetrahedral intermediate. Gln23ß is also shown to interact with the nucleophilic part of a substrate and contribute to the stabilization of the tetrahedral intermediate.

The PGA^{A} from the mutant strain *Achromobacter* sp. CCM 4824 [10] has been firstly characterized by Škrob et al. [11]. Molecular mass of α-subunit and β-subunit is 27.0 and 62.5 kDa, respectively.

Abbreviation: *N*-PhAc-amino acid, *N*-phenylacetyl amino acid.

* Corresponding author at: Laboratory of Enzyme Technology, Institute of Microbiology,v.v.i., Academy of Sciences of the Czech Republic, Vídeňská 1083, 142 20 Prague 4, Czech Republic. Fax: +420 296442347.
E-mail address: grulich@biomed.cas.cz (M. Grulich).

http://dx.doi.org/10.1016/j.molcatb.2015.09.008
1381-1177/

The results showed that the enzyme is more efficient biocatalyst in comparison with PGA^{Ec} as regards syntheses of semi-synthetic β-lactam antibiotics. Its potential for kinetically controlled syntheses of semisynthetic β-lactam antibiotics has been shown recently [12] and has already been used at industrial scale by Fermenta Biotech Ltd.

Here we present results of the research into enantioselectivity of PGA^{A}. First, the enantioselective resolutions of racemic mixtures of α/β-amino acids having considerable potential for pharmaceutical applications were determined experimentally. Then we describe a construction of a homology model of PGA^{A} and consequent molecular docking experiments employed to understand molecular basis of PGA^{A} enantioselectivity. Experimentally validated model of the enzyme was used to predict PGA^{A} enantioselectivity towards new, hitherto non-investigated substrates.

2. Experimental

2.1. Microorganisms and culture conditions

Recombinant strain *E. coli* BL21(pKX1P1) and *E. coli* RE3(pKA18) was used to prepare biomass for purification of PGA^{A} and PGA^{Ec}, respectively. Fed batch cultures of the strains in a stirred bioreactor were described earlier [13,14].

2.2. Enzyme purification and hydrolytic activity assay

PGA^{A} was purified as described by Škrob et al. [11] and PGA^{Ec} according to Kutzbach and Rauenbusch [15]. Purified PGA^{Ec} and PGA^{A} has the specific activity of 60 and 50 U/mg protein, respectively. The activity of 1 unit (U) was defined as the amount of an enzyme producing 1 μmol of phenyl acetic acid per minute from PenG (2% w/v) in 0.05 M sodium phosphate buffer (pH 8.0) at 37 °C.

2.3. Chemical synthesis of N-phenylacetyl-amino acid racemic mixtures

Phenylacetyl chloride (0.044 mol) was added dropwise to 100 mL of NaOH solution (10%, w/v) of racemic mixture of an amino acid (0.04 mol) kept on ice bath. The reaction mixture was acidified to pH 2 with 6 M HCl, and *N*-phenylacetyl amino acid (*N*-PhAc amino acid) was extracted three times with ethyl acetate and recrystallized from the ethyl acetate solution. Purity of the product was determined by HPLC using C-8 reverse phase column. Eluent consisted of H_2O (containing 0.1% TFA): acetonitrile in ratio 7:3. For more details on products yields, chemical shifts in the ^{1}H NMR and ^{13}C NMR spectra and data from MS analyses see Supplementary data (Figs. S1–S7).

2.4. Enantioselective hydrolysis of N-PhAc-amino acid racemic mixtures

The reactions were carried out in a pH-stat at 30 °C under continuous stirring. A water solution (25 mL) containing 0.025 M *N*-PhAc-amino acid racemic mixture was incubated at pH 7.5 for 30 min. 50 U of PGA^{Ec} or PGA^{A} were added to the reaction mixture and the pH was maintained at 7.5 by titration (2 M NH_4OH).

Concentrations of reactants were analyzed by HPLC using Dionex P580 Pump, C-8 column and a Dionex PDA-100 detector set at 215 nm. The mobile phase consisted of a mixture of acetonitrile: water (containing 0.1% TFA) = 3: 7.

The enantiomeric excess of the products (ee_p) was determined by HPLC using Dionex P580 Pump, Sumichiral OA 5000 column and UV detector set at 215 nm or Daicel Crownpak CR(+) column using the Dionex PDA-100 detector set at 200 nm. Composition of eluent solution was as follows: for Sumichiral OA 5000 column (flow rate of 0.4 mL/min)—2 mM $CuSO_4$ containing 5% or 2% isopropanol; for Daicel Crownpak CR(+) column (flow rate of 1 mL/min)—aqueous solution of $HClO_4$ (pH 1) containing methanol (10% v/v). Retention times of enantiomers of reaction products are summarized in Supplementary data (Table S1).

E values describing enantioselectivities of PGA^{Ec} or PGA^{A} were determined using Eq. (1):

$$E = \frac{\ln\left(A/A_0\right)}{\ln\left(B/B_0\right)} \quad (1)$$

where A_0 and A represent the concentrations of the faster reacting enantiomer at the reaction times 0 and t, resp. B_0 and B denote the concentrations of the slower reacting enantiomer at the reaction times 0 and t, resp. [16]. The enantiomeric ratio E was also determined by non-linear regression using Eq. (2) which is derived from Sihí's equation describing a relationship between E, degree of conversion (c) and the enantiomeric excess ee_p [16].

$$c = 1 - \left(\left(1 + ee_p\right) \times \left(1 - ee_p\right)^{-E}\right)^{1/(E-1)} \quad (2)$$

2.5. Molecular modeling

A homology model of PGA^{A} was prepared using the sequence of amino acids from GenBank (AAY25991). The most suitable template for modeling was identified by PSI-BLAST search using the ExPaSy server against sequences in the Protein Data Bank. The PGA^{A} query sequence was then aligned with the best template—PGA^{Ec} enzyme (PDB-ID 1GM7, sequence identity 50%) using ClustalOmega [17]. Identity of amino acid residues forming the active site between the template and the query was 88%. Only two substitutions occurred within the seventeen amino acid residues forming the active site (Val56ß → Leu56ß and Ser149α → Ala149α), and no insertions or deletions were observed for these positions. Alignments were prepared with a constraint between the Ser1β residue of the query sequence and the corresponding serine residue of the template. The homology modeling based on alignment of PGA^{A} and PGA^{Ec} was performed using the Swiss-model webserver [18]. The α and β chains of penicillin acylases were modelled separately by calculating a number of minimized intermediate models which were ranked by the structure quality Z-score. One model of the α chain and one of the β chain had to be chosen from this ensemble of structures, not only on the basis on the Z-score, but also by taking into account the reciprocal positions of the two chains. The final model was evaluated using a program Verify 3D [19] with the template validation data used as the baseline to assess the respective models. To facilitate reproducibility of the work, the model was deposited to Protein Model DataBase [20] under the following access code PM0080082. The analysis of Ramachandran plot generated by RAMPAGE server [21] suggested a high quality of the homology model with more than 95% of residues located in the favored region, for detailed report from the analysis see Supplementary data (Fig. S8). This finding was further confirmed by low Z-score of −0.29 reported by QMEAN server [22,23] indicating that the quality of the model is comparable to the high-resolution crystal structures of proteins of similar size. Next, the PGA^{A} model was protonated *via* H++ server at pH 7.5 using default settings. Protonation of catalytically important amino acid residues was modified manually so that they conform to specific reaction mechanism, *i.e.*, enantioselective hydrolysis of *N*-PhAc-α/β-amino acids [24].

Molecular docking calculations were performed through AutoDock Vina plug-in for PyMol [25]. Structures of substrates were prepared using Avogadro molecular editor [26] and energetically minimized in four steps of the steepest descent using MMFF94 force field [27]. Substrate and protein structures were converted to AutoDock Vina compliant format by AutoDock Vina

plug-in for PyMol. For docking, the grid box (22.5 × 22.5 × 22.5 Å) covering the PGA^A active site was defined and centered on the center of mass of Ser1β, Ala69β and Asn241β residues. The docking calculations were performed using Autodock Vina software [28] with an exhaustiveness of 200, maximum of 9 generated binding modes and maximum energy difference between the best and the worst binding modes of 3 kcal/mol. Visualization of docked binding modes and analysis of its geometries were performed in PyMol [29] software. Mechanism-based geometric criteria for prediction of substrate reactivity [30] were derived accordingly to the catalytic mechanism of PGAs. To evaluate reactivity of docked substrate conformations, the binding modes were assessed by using following criteria: (i) distance between nucleophilic oxygen atom O$^\gamma$ of Ser1β and attacked carbon from carbonyl group of the substrate reflecting the probability of nucleophilic attack, (ii) lengths of hydrogen bonds between nitrogen atoms from amino groups of Ala69β and Asn241β and the oxygen atom from the carbonyl group of substrate that stabilize the negative charge of the reactive tetrahedral intermediate, and (iii) length of hydrogen bond between oxygen atom from carbonyl group of Gln23β and leaving nitrogen group of substrate that also contributes to the stabilization of the tetrahedral intermediate (Fig. 1). To derive particular cutoff distances for these criteria, high-quality structures of PGA complexed with substrates and their analogs were analyzed (Supplementary data, Table S2). Since such evaluation provides only qualitative two-state prediction of substrates reactivity—reactive and non-reactive, we can accurately predict only potential for highly enantioselective discrimination. In such a case, one enantiomer is predicted as poorly active, while the other one as well active. It is important to note that minor differences in enantioselectivity cannot be predicted using employed approach. Additionally, the interactions present in predicted binding modes were analyzed by PoseView [31].

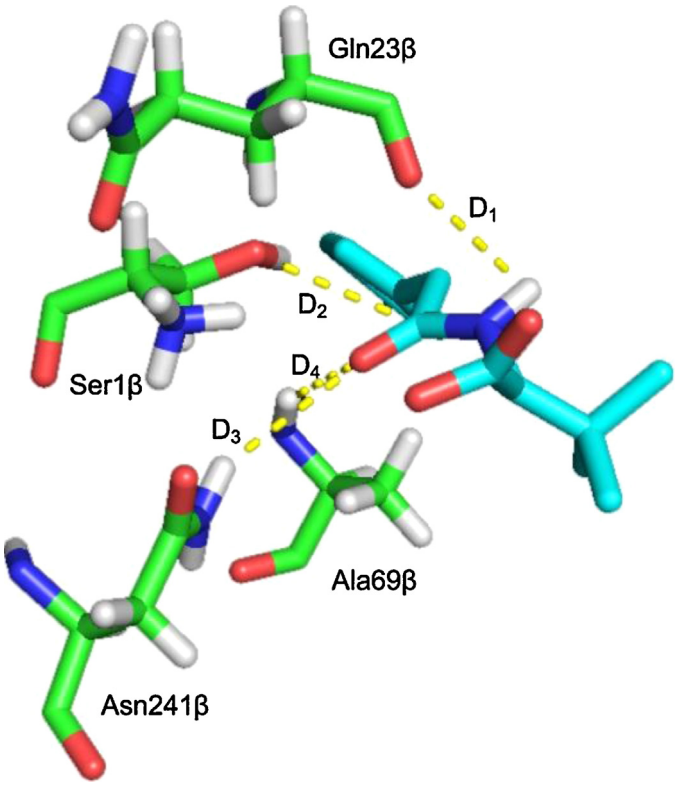

Fig. 1. Mechanism-based geometric criteria developed for evaluation of reactivity of docked substrates in active site of PGA^A. The essential amino acid residues of *PGA^A*'s active site are shown as green sticks. Binding mode of (*S*)-*N*-PhAc-*tert*-leucine is shown as cyan sticks. The analyzed distances D_1 ($O^{Gln23\beta} \rightarrow H$), D_2 ($O^{Ser1\beta} \rightarrow C$), D_3 ($N^{Asn241\beta} \rightarrow O$) and D_4 ($N^{Ala69\beta} \rightarrow O$) are displayed as yellow dashed lines. (For interpretation of the references to colour in this figure legend, the reader is referred to the web version of this article.)

3. Results and discussion

3.1. Experimental determination of enantioselectivity of PGA^A

Research into enantioselectivity of PGAs started in 60s of the last century and dealt mainly with resolutions of racemic mixtures of α-amino acids and their derivatives [32,33]. So far, main concern on PGA^A dealt with syntheses of several important semi-synthetic β-lactam antibiotics. In order to asses a broader potential of PGA^A, we have focused on seven α/β-amino acids (Table 1) that have application potential as building blocks of active pharmaceutical ingredients. These substrates were used to compare enantioselec-

Table 1
Substrates subjected to biocatalysis by PGA^A and PGA^{Ec}.

Substrates	Structure	Product application	References
N-PhAc-α-phenylalanine	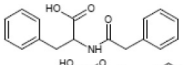	α-(*S*)-phenylalanine—direct precursor of neuromodulator phenylethylamine	[35]
N-PhAc-α-homophenylalanine	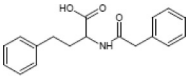	(*S*)-homophenylalanine—building block of drugs for threatment of hypertension and cardiovascular diseases	[36]
N-PhAc-β-leucine	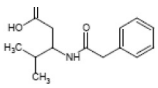	Building block for terpenoids or proteins	[37]
N-PhAc-α-leucine	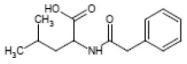	(*S*)-enantiomer—building block of proteins	[38]
N-PhAc-α-isoleucine	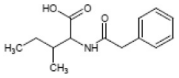	(*S*)-isoleucine—food complement	
N-PhAc-β-homoleucine	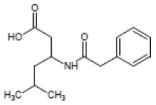	Enhancer of activity of myeloperoxidase, building block of biologically active tripeptides	[39,40]
N-PhAc-α-*tert*-leucine	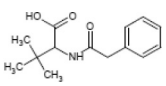	(*S*)-*tert*-leucine - building block for anti-AIDS and anti-cancer pharmaceuticals	[24,41]

Table 2
Experimentally determined enantioselectivity of PGA^{A} and PGA^{Ec} towards *N*-PhAc-α/β-amino acids.

Substrate	*E*-values	
	PGA^{A}	PGA^{Ec}
N-PhAc-α-phenylalanine	90 ± 5	90 ± 5
N-PhAc-α-homophenylalanine	80 ± 5	80 ± 5
N-PhAc-β-leucine	68 ± 3	60 ± 5
N-PhAc-α-leucine	80 ± 5	80 ± 5
N-PhAc-α-isoleucine	80 ± 5	80 ± 5
N-PhAc-β-homoleucine	85 ± 4	55 ± 5
N-PhAc-α-*tert*-leucine	105 ± 5	75 ± 5

tivities of PGA^{A} with PGA^{Ec}, an enzyme exhibiting 50 % sequence identity with PGA^{A} [34].

Racemates of substrates listed in Table 1 were used in enantioselective hydrolytic reactions catalyzed by purified PGA^{Ec} and PGA^{A} and their enantioselectivity values (*E*) were determined using HPLC analysis (Table 2). A high degree of enantioselectivity ($E = 90 \pm 5$) for both PGA^{A} and PGA^{Ec} was observed in enzyme-catalyzed hydrolyses of *N*-PhAc-α-phenylalanine. Both PGA^{A} and PGA^{Ec} exhibited similar degree of enantioselectivity towards substrate *N*-PhAc-α-leucine and *N*-PhAc-α-isoleucine. On the other hand, PGA^{A} exhibited markedly higher enantioselectivity (in descending order) with: *N*-PhAc-β-homoleucine, *N*-PhAc-α-*tert*-leucine and *N*-PhAc-β-leucine (Table 2).

3.2. Structural basis of enantioselectivity of PGA^{A}

A lot of effort has been invested into the structural analysis of PGAs and understanding of its substrate-enzyme interactions. Amino acid residues Ser1β, Gln23β, Ala69β and Asn241β [42] are recognized as essential amino acid residues of aminic subsite in the eleven PGAs so far characterized [5]: Ala69β and Asn241β participate in formation of "oxyanion - hole", Gln23β stabilizes E-S tetrahedral intermediate and the Ser1β residue serves as a catalytic residue. It is proposed that the general topology and the quarternary structure of the active site cavity might be conserved throughout the PGA family [43]. However, slight variations in amino acid residues are evident in the acyl binding subsite that is formed in *E. coli* by Met142α, Arg145α, Phe146α, Phe24β, Thr32β, Pro49β, Val56β, Trp154β, and Ile177β [42,44]. Due to so far unsuccessful effort to crystallize the PGA^{A} (data not shown), we decided to prepare homology model of PGA^{A} to study molecular mechanism beyond enantioselectivities of this enzyme.

The model of PGA^{A} was used as a receptor in molecular docking experiments with both enantiomeric forms of seven substrates studied experimentally (Table 1). The binding energies predicted by molecular docking strongly correlated ($R = -0.76$) with the molecular weight of investigated substrates. However, the largest difference in the predicted binding energies between enantiomers of a given substrate was 0.7 kcal/mol only (Table S3). Since such difference is within the error margin of the scoring function, the observed difference between binding affinities of individual enantiomers should be considered as negligible without any significant influence on the enantioselectivity of PGA^{A}. The predicted structures of complexes were further analyzed in respect to the interactions of substrates with amino acid residues involved in the catalysis (*i.e.*, Ala69β, Asn241β, Gln23β and Ser1β). For all *N*-PhAc-α-amino acids and *N*-PhAc-β-homoleucine, the distances from functional groups of important amino acid were markedly shorter for (*S*)-enantiomer which predicted this enantiomer as the preferred form (Table 3). On the contrary, (*R*)-*N*-PhAc-β-leucine was preferred enantiomer. Acyl moieties of all enantiomer pairs adopted binding modes that allowed the moiety to fit in the acyl-binding site of PGA^{A}, in which their phenyl rings formed π–π interactions with Phe24β and most frequently also hydrophobic interactions with Phe24β, Thr68β and Ala69β, see Supplementary data (Figs. S9 and S10). Based on our docking experiments we recognized, in addition to acyl binding subsite, also the "secondary hydrophobic" subsite formed mainly by the following amino acid residues: Ala69β, Phe71β, Ala149α and Phe146α.

Two mechanisms of PGA^{A}'s enantioselectivity may be recognized accordingly to the bulkiness of substrate's substituent.

3.3. Enantioselectivity mechanism adopted by substrates with bulky substituents

N-PhAc-α-phenylalanine, *N*-PhAc-α-homophenylalanine, *N*-PhAc-α-isoleucine, and *N*-PhAc-α-*tert*-leucine all adopted similar binding mode in the aminic subsite without exception (Fig. 2A). The bulky, hydrophobic nucleophilic substituents were all oriented to the secondary hydrophobic subsite. In the case of *N*-PhAc-α-phenylalanine and *N*-PhAc-α-homophenylalanine containing the second aromatic ring in the structure of their nucleophilic substituents, additional π–π and hydrophobic interactions were formed between this ring and either with Phe71β or Phe146α residues within this site see Supplementary data (Fig. S9). The carboxyl moieties of all four substrates were oriented towards part of the active site with positively charged and hydrophilic amino acid residues (*e.g.*, Arg263β, Ser390β, Asn214β and N-terminal part of Ser1β). Oxygens from the carbonyl group of (*S*)-enantiomers were always properly stabilized by amino acid residues of the "oxyanion-hole" in the orientation enabling nucleophilic attack upon the

Table 3
Reactivity of binding modes of α/β-amino acids in PGA^{A}. Disfavoring interactions beyond the cutoff values are highlighted in bold.

Substrate	Enantiomer	Distance (Å)				Predicted as reactive	Predicted preference
		$O^{Ser1\beta} \rightarrow C$	$N^{Ala69\beta} \rightarrow O$	$N^{Asn241\beta} \rightarrow O$	$O^{Gln23\beta} \rightarrow H$		
N-PhAc-α-phenylalanine	(*S*)	3.4	4.0	4.0	3.9	Yes	(*S*)
	(*R*)	**5.2**	**6.3**	**7.9**	**5.4**	No	
N-PhAc-α-homophenylalanine	(*S*)	3.3	3.7	3.9	3.3	Yes	(*S*)
	(*R*)	**4.6**	**6.2**	**7.4**	**5.2**	No	
N-PhAc-β-leucine	(*R*)	3.2	3.7	4.0	3.5	Yes	(*R*)
	(*S*)	3.4	3.9	4.0	**4.4**	No	
N-PhAc-α-leucine	(*S*)	3.4	3.9	3.8	3.0	Yes	(*S*)
	(*R*)	3.4	4.0	4.1	**4.6**	No	
N-PhAc-α-isoleucine	(*S*)	3.6	4.1	3.9	2.8	Yes	(*S*)
	(*R*)	**4.5**	**6.2**	**7.4**	**5.1**	No	
N-PhAc-β-homoleucine	(*S*)	3.2	3.8	3.7	2.9	Yes	(*S*)
	(*R*)	3.4	3.8	4.0	**4.4**	No	
N-PhAc-α-*tert*-leucine	(*S*)	3.3	4.0	4.1	3.3	Yes	(*S*)
	(*R*)	**4.7**	**6.3**	**7.5**	**4.8**	No	

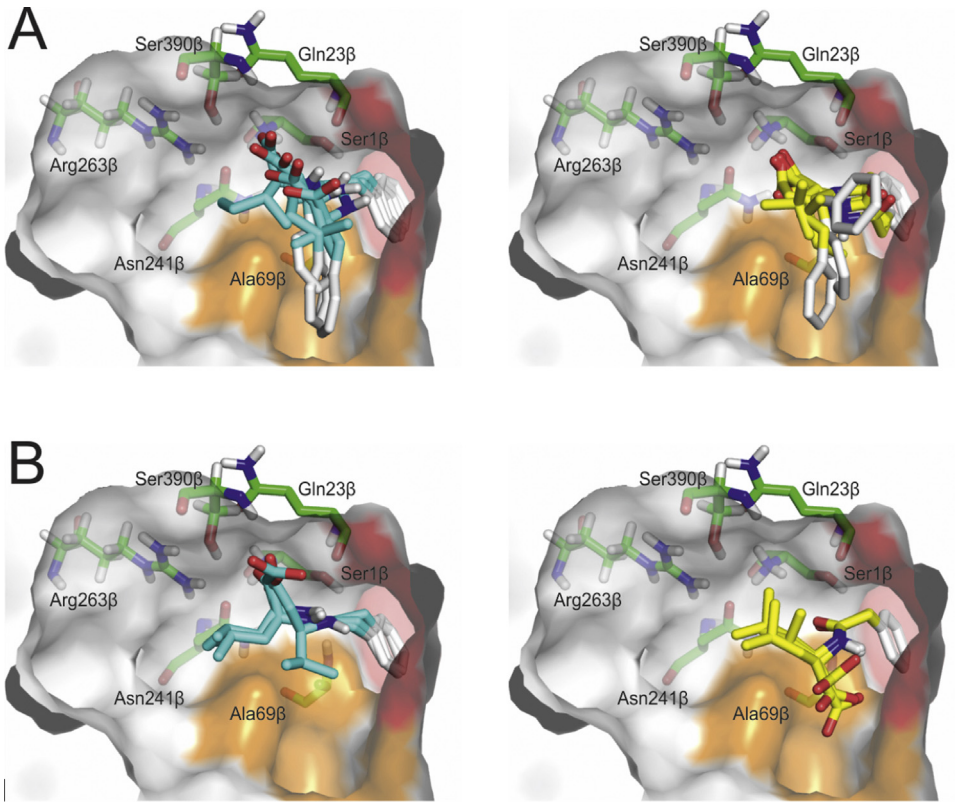

Fig. 2. Predicted binding modes of seven experimentally tested substrates within the active site cavity of PGA^A. (A) Binding modes of enantiomers with bulky substituents (moieties: α-phenylalanine, α-homophenylalanine, α-isoleucine, and α-*tert*-leucine). (B) Binding modes of enantiomers with less bulky substituents. Grey surface—the active site cavity; red surface—the acyl-binding subsite; orange surface—the secondary hydrophobic subsite. Crucial catalytic amino acid residues of the active site are green; preferred and non-preferred enantiomers are cyan and yellow, respectively. (For interpretation of the references to colour in this figure legend, the reader is referred to the web version of this article.)

carbon atom of the carbonyl by Ser1β. Also hydrogens from amino groups of substrates were properly stabilized by Gln23β. On the contrary, binding modes of (*R*)-enantiomers had their peptide bonds oriented in the opposite direction (Fig. 2A). This orientation resulted into larger spatial separation of substrates' carbonyl oxygen and hydrogen of stabilizing functional amino group of the enzyme. Such binding modes also effectively shielded the attacked carbon from the nucleophilic attack by Ser1β. All this facts combined suggest that (*R*)-enantiomers of this group of substrates were poorly reactive at best, while (*S*)-enantiomers of these compounds were better stabilized for reaction as is illustrated by all four measured distances being much shorter contributing to its predicted preference (Table 3).

3.4. Enantioselectivity mechanism adopted by substrates with less bulky substituents

This group of substrates includes *N*-PhAc-β-homoleucine, *N*-PhAc-α-leucine and *N*-PhAc-β-leucine. The binding modes of (*S*)-enantiomers of *N*-PhAc-β-homoleucine and *N*-PhAc-α-leucine followed the scheme for substrates with the bulky substituents (Fig. 2B), with the exception that these substituents were not oriented towards the secondary hydrophobic subsite of the binding cavity. The predicted binding modes of these two (*S*)-enantiomers fulfilled all criteria for their reactivity (Table 3).

In the case of (*R*)-enantiomers of *N*-PhAc-β-homoleucine and *N*-PhAc-α-leucine, the carboxyl groups pointed towards the secondary hydrophobic subsite and simultaneously their non-polar substituents pointed towards the positively charged and hydrophilic residues (Fig. 2B). These binding modes allowed the peptide bonds of (*R*)-enantiomers of *N*-PhAc-β-homoleucine and *N*-PhAc-α-leucine to adopt similar orientation as (*S*)-enantiomers of *N*-PhAc-β-homoleucine and *N*-PhAc-α-leucine and therefore to partially restore necessary stabilization of their carbonyl oxygens by the residues of the "oxyanion-hole" and orientation of attacked carbon towards catalytic nucleophile (Table 3). However, the amino groups of substrates were not stabilized by Gln23β, and the obviously non-complementary interactions required by these binding modes should further disfavor their formation. In the case of *N*-PhAc-β-leucine racemic mixture, binding modes of both enantiomers followed the same pattern as described above but (*R*)-enantiomer was the preferred form (Table 3).

3.5. Prediction of enantioselectivity of PGA^A towards new substrates

Since the molecular docking of seven substrates into the homology model of PGA^A confirmed experimental results obtained with purified PGA^A (Table 2), we employed this approach for *in-silico* prediction of enantioselective hydrolyses of non-conventional α/β-amino acid enantiomers of which have an application potential (Table 4). We should stress here that enantioselective hydrolyses of majority of racemates of these substrates catalyzed by so far characterized PGAs have not yet been reported. A reference to stereoselectivity of PGA with *N*-PhAc-3-aminopent-4-ynoic acid derivative and *N*-PhAc-*p*-Cl-β-phenylalanine can be found in research studies [45,46].

Results of docking experiments with pure enantiomers of racemates of seven *N*-PhAc-α/β-amino acids into active site cavity of homology model of PGA^A are shown in Table 5.

Similarly to previous analysis, both enantiomers exhibited comparable binding energies ruling out a differential binding as a source

Table 4
Novel substrates used for prediction of PGA^A enantioselectivity.

Substrates	Structure	Product application	References
N-PhAc-3-aminopent-4-ynoic acid	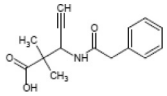	(*S*)-enantiomer—building block of Elarofiban	[47]
N-PhAc-3-amino-3-pyridin-propanoic acid	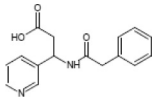	(*S*)-enantiomer—building block for Xemilofiban	[48]
N-PhAc-3-amino-3-benzyl-2-hydroxybutanoic acid	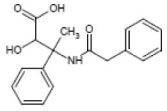	(*S*)-enantiomer—building block for Paclitaxel	[49]
N-PhAc-3-amino-3-(3-chloro-4,5-dihydroxyphenyl) propanoic acid	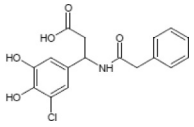	(*S*)-enantiomer—building block of Lidamycin	[50]
N-PhAc-*p*-Cl-α-phenylalanine	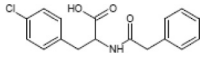	(*S*)-enantiomer—precursor for synthesis of analgesic Zolmitriptan	[51]
N-PhAc-*p*-F-α-phenylalanine	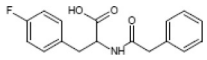	(*R*)-enantiomer—building block of Abarelix	[51]
N-PhAc-*p*-Cl-β-phenylalanine	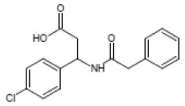	(*S*)-enantiomer market product	Sigma–Aldrich

of potential enantiopreference of PGA^A (Table S3). Therefore we further focused on evaluation of differences in potential reactivity of these novel substrates using validated geometric criteria. As shown for α/β-amino acids, such analysis was able to successfully predict high enantioselectivity in cases, when reactivity of one enantiomer was seriously disfavored. Based on this analysis, we predicted high enantiopreference of PGA^A for three (*R*)-enantiomers and two (*S*)-enantiomers of novel substrates (Table 5). However, we could not entirely exclude possibility of moderate-to-low enantioselectivity for remaining two substrates. In the case of *N*-PhAc-3-aminopent-4-ynoic acid, binding of its rigid and extended ethynyl group into the secondary hydrophobic subsite of the PGA^A prevented stabilization of carbonyl oxygen of both enantiomers by the residues of "oxyanion hole" as well as proper stabilization by interactions with Gln23β, predicting both enantiomers as inactive or poorly active. The binding modes of (*R*)-enantiomers of both *N*-PhAc-3-amino-3-pyridin-propanoic acid and *N*-PhAc-3-amino-3-(3-chloro-4,5-dihydroxyphenyl) propanoic acid had their aromatic nucleophilic substituents located in the secondary hydrophobic subsite as was the case of the binding modes for the group of substrates containing bulkier substituents. Interestingly, the (*S*)-enantiomers of these compounds were bound with their carboxyl groups in the secondary hydrophobic subsite, while their aromatic nucleophilic substituents pointed towards hydrophilic part of the active site in the same fashion as the group of substrates containing less bulky substituents. Since the aromatic substituents of these two substrates carry also some polar groups, their binding modes seemed to be relatively easy to accommodate into the

Table 5
In-silico prediction of enantioselective hydrolyses of novel substrates catalyzed by PGA^A. Disfavoring interactions beyond the cutoff values are highlighted in bold.

Substrate	Enantiomer	Distance (Å)				Predicted as reactive	Predicted preference
		$O^{Ser1\beta} \rightarrow C$	$N^{Ala69\beta} \rightarrow O$	$N^{Asn241\beta} \rightarrow O$	$O^{Gln23\beta} \rightarrow H$		
N-PhAc-3-aminopent-4-ynoic acid	(*R*)	**3.9**	**4.5**	**4.7**	**4.7**	No	–
	(*S*)	3.5	**4.4**	**4.3**	**5.3**	No	
N-PhAc-3-amino-3-pyridin-propanoic acid	(*R*)	3.2	3.7	3.9	3.1	Yes	(*R*)
	(*S*)	**4.2**	**4.2**	**5.0**	**5.0**	No	
N-PhAc-3-amino-3-benzyl-2-hydroxybutanoic acid	(*S*)	3.3	3.8	4.0	3.4	Yes	(*S*)
	(*R*)	**4.2**	**6.1**	**7.8**	3.8	No	
N-PhAc-3-amino-3-(3-chloro-4,5-dihydroxyphenyl) propanoic acid	(*R*)	3.1	3.6	4.0	2.9	Yes	(*R*)
	(*S*)	3.6	4.1	**4.3**	4.2	No	
N-PhAc-*p*-Cl-α-phenylalanine	(*S*)	3.2	3.8	3.8	2.0	Yes	(*S*)
	(*R*)	**4.8**	**6.6**	**8.0**	4.2	No	
N-PhAc-*p*-F-α-phenylalanine	(*R*)	3.6	4.1	4.0	2.6	Yes	–
	(*S*)	3.4	4.0	4.1	3.7	Yes	
N-PhAc-*p*-Cl-β-phenylalanine	(*R*)	3.2	3.6	4.0	3.2	Yes	(*R*)
	(*S*)	**4.4**	**6.7**	**7.9**	3.4	No	

PGA^A's binding site. In any case observed binding modes of (*S*)-enantiomers provided poor interactions with all four functionally important residues (Table 5). This analysis suggested high enantiopreference towards (*R*)-enantiomers of these two substrates. In the case of *N*-PhAc-3-amino-3-benzyl-2-hydroxybutanoic acid, both enantiomers complied to the binding modes observed for group of substrates having the bulky substituent, with the exception that hydroxyl group of (*S*)-enantiomer took over the interaction of carboxyl group with hydrophilic part of the active site cavity. Nevertheless, a difference in measured distances indicated strong (*S*)-preference (Table 5). Substrates *N*-PhAc-*p*-Cl-α-phenylalanine and *N*-PhAc-*p*-Cl-β-phenylalanine fully followed behavior of the group of substrates containing bulkier substituents including predicted enantiopreference towards their (*S*)- and (*R*)-enantiomers, respectively. Enantiomers of *N*-PhAc-*p*-F-α-phenylalanine adopted extended conformations because their nucleophilic substituents could fit better into aminic subsite being possibly stabilized by π–π interactions with Phe71β. Although the carboxyl group of (*R*)-enantiomer was being oriented into the secondary hydrophobic subsite, the distances to interacting groups were favorable for both enantiomers predicting their good reactivity (Table 5). Therefore, no conclusion on possible enantioselectivity of PGA^A towards this substrate could be drawn.

4. Conclusions

In this study, we present results of the research into enantioselectivity potential of a novel industrial catalyst PGA^A towards racemic mixtures of α/β-amino acids, pure enantiomers of which have an application in pharmaceutical industry. We have demonstrated that PGA^A exhibited markedly higher enantioselectivity than PGA^{Ec} (in descending order) with: *N*-PhAc-β-homoleucine, *N*-PhAc-α-*tert*-leucine, and *N*-PhAc-β-leucine. We have constructed a homology model of PGA^A using availability of a crystal structure of PGA^{Ec}. We were able to evaluate plausibility of the model by using molecular docking calculations: the results of molecular modeling were identical with the enantiopreference of PGA^A found for all experimentally studied substrates. Follow-up docking experiments with seven non-conventional *N*-PhAc-α/β-amino acids enabled us to predict the enzyme enantiopreference for most of these substrates. Predictions indicated high PGA^A's enantiopreference for (*R*)-enantiomers of three compounds and (*S*)-enantiomers of two substrates. *In-silico* prediction of enantiopreference revealed PGA^A convenience towards production of (*S*)-enantiomer of *N*-PhAc-3-amino-3-benzyl-2-hydroxybutanoic acid, a potential building block for paclitaxel. *In-silico* prediction of PGA^A's enantiomer preference could be powerful tool for selection of compounds that are not available on the market but can serve as a source of chiral compounds for pharmaceutical industry.

Ethical

The authors are aware of ethical standards and declare that they have no conflicts of interests. The research does not involve human being or animals.

Aknowledgements

This publication is supported by the project "BIOCEV - Biotechnology and Biomedicine Centre of the Academy of Sciences and Charles University"(CZ.1.05/1.1.00/02.0109), from the European Regional Development Fund, by long-term research development project RVO 61388971 of the Institute of Microbiology, the project SVV 260079/2014 and partially sponsored by Fermenta Biotech Ltd., India. Work of JB was supported by the "Employment of Best Young Scientists for International Cooperation Empowerment" (CZ.1.07/2.3.00/30.0037) project co-financed by the European Social Fund and the state budget of the Czech Republic.

Special thanks to Peter Babiak for discussion on organic syntheses and to Eva Šebestová on homology model construction.

Appendix A. Supplementary data

Supplementary data associated with this article can be found, in the online version, at http://dx.doi.org/10.1016/j.molcatb.2015.09.008.

References

[1] M. Arroyo, I. de laMatta, C. Acebal, M. Pillar Castillon, Appl. Microbiol. Biotechnol. 60 (2003) 507–514.
[2] A.K. Chandel, L.V. Rao, M.L. Narasu, O.V. Singh, Enzyme Microb. Tech. 42 (2007) 199–207.
[3] R.P. Elander, Appl. Microbiol. Technol. 61 (2003) 385–392.
[4] C.F. Sio, W.J. Quax, Curr. Opin. Biotechnol. 15 (2004) 349–355.
[5] M. Grulich, V. Štěpánek, P. Kyslík, Biotechnol. Adv. 31 (2013) 1458–1472.
[6] A. Basso, P. Braiuca, S. Clementi, C. Ebert, L. Gardossi, P. Linda, J. Mol. Catal. B Enzyme 19–20 (2002) 423–430.
[7] H.J. Duggleby, S.P. Tolley, C.P. Hill, E.J. Dodson, G. Dodson, P.C.E. Moody, Nature 373 (1995) 264–268.
[8] R.C. Giordano, M.P. Ribeiro, R.L. Giordano, Biotechnol. Adv. 24 (2006) 27–41.
[9] K. Srirangan, V. Orr, L. Akawi, A. Westbrook, M. Moo-Young, C. Perry Chou, Biotechnol. Adv. 31 (2013) 1319–1332.
[10] K. Plháčková, S. Bečka, F. Škrob, P. Kyslík, Appl. Microbiol. Biotechnol. 62 (2003) 507–516.
[11] F. Škrob, S. Bečka, K. Plháčková, V. Fotopulosová, P. Kyslík, Enzyme Microb. Tech. 32 (2003) 738–744.
[12] S. Bečka, V. Štěpánek, R.W. Vyasarayani, M. Grulich, J. Maršálek, K. Plháčková, M. Dobišová, H. Marešová, M. Plačková, R. Valešová, A. Palyzová, A. Datla, T.K. Ashar, P. Kyslík, Appl. Microbiol. Biotechnol. 98 (2014) 1195–1203.
[13] L. Sobotková, V. Štěpánek, K. Plháčková, P. Kyslík, Enzyme Microb. Tech. 19 (1996) 389–397.
[14] P. Kyslík, V. Štěpánek, L. Hollerová, S. Bečka, W.R., Vyasarayani, A., Datla, K. Plháčková, J. Maršálek US patent 8039604B2, 2011 Oct 18.
[15] C. Kutzbach, E. Rauenbusch, Hoppe-Seyler's Z. Physiol. Chem. 354 (1974) 45–53.
[16] C.S. Chen, Y. Fujimoto, G. Girdaukas, C.J. Sih, J. Am. Chem. Soc. 104 (1982) 7294–7299.
[17] J.D. Thompson, D.G. Higgins, T.J.W. Gibson, Nucleic Acids Res. 22 (1994) 4673–4680.
[18] K. Arnold, L. Bordoli, J. Kopp, T. Schwede, Bioinformatics 22 (2006) 195–201.
[19] J.U. Bowie, R. Luthy, D. Eisenberg, Science 253 (1991) 164–170.
[20] T. Castrignanò, P.D. De Meo, D. Cozzetto, I.G. Talamo, A. Tramontano, Nucleic Acids Res. 34 (2006) 306–309.
[21] S.C. Lovell, I.W. Davis, W.B. Arendall III, P.I.W. de Bakker, J.M. Word, M.G. Prisant, J.S. Richardson, D.C. Richardson, Proteins Struc. Funct. Genet. 50 (2002) 437–450.
[22] P. Benkert, M. Künzli, T. Schwede, Nucleic Acids Res. 37 (2009) 510–514.
[23] P. Benkert, M. Biasini, T. Schwede, Bioinformatics 27 (2011) 343–350.
[24] S.-L. Liu, Q.-X. Song, D.-Z. Wei, Y.-W. Zhang, X.-D. Wang, Prep. Biochem. Biotechnol. 36 (2006) 235–241.
[25] D. Seeliger, B.L. deGroot, J. Comput. Aided Mol. Des. 24 (2010) 417–422.
[26] M.D. Hanwell, D.E. Curtis, D.C. Lonie, T.M. Vandermeersch, E. Zurek, G.R. Hutchinson, J. Cheminform. 1 (2012) 4–17.
[27] T.A. Halgren, J. Comput. Chem. 17 (1996) 490–519.
[28] O. Trott, A.J. Olson, J. Comput. Chem. 31 (2010) 455–461.
[29] The PyMOL Molecular Graphics System [computer program]. Version 1.4, DeLano Scientific, San Carlos, CA, USA, 2004.
[30] L. Daniel, T. Buryska, Z. Prokop, J. Damborsky, J. Brezovsky, J. Chem. Inf. Model. 55 (2015) 54–62.
[31] K. Stierand, P. Maaß, M. Rarey, Bioinformatics 22 (2006) 1710–1716.
[32] M. Cole, Biochem. J. 115 (1969) 741–745.
[33] G. Lucente, A. Romeo, D. Rossi, Experientia 21 (1965) 317–318.
[34] S.E. McVey, M.A. Walsh, G.G. Dodson, K.S. Wilson, J.A. Brannigan, J. Mol. Biol. 313 (2001) 139–150.
[35] M.D. Berry, J. Neurochem. 90 (2004) 257–271.
[36] A.L. Ahmad, P.C. Oh, S.R.A. Ahukor, Biotechnol. Adv. 27 (2009) 286–296.
[37] G.C. Barrett, Chemistry and Biochemistry of the Amino Acids, Chapmann and Hall, 1985.
[38] L. Breen, T.A. Churchward-Venne, J. Physiol. 590 (9) (2012) 2065–2066.
[39] W. Haag, S., Becquerelle, S., Valvani, O. Abril-Horpel, EP patent 2296693A1, 2012 Mar 7.
[40] D. Seebach, J.L. Matthews, Chem. Commun. (1997) 2015–2022.
[41] A.S. Bommarius, M. Schwam, K. Stingl, M. Kottenhahn, K. Huthmacher, K. Drauz, Tetrahedron Asymmetr. 6 (1995) 2851–2888.
[42] B. Oh, K. Kim, J. Park, J. Hoon, D. Han, Y. Kim, Biochem. Biophys. Res. Commun. 319 (2004) 486–492.

[43] J.L. Barbero, J.M. Buesa, G.G. deBuitrago, E. Mendez, A. Pez-Aranda, J.L. Garcia, Gene 49 (1986) 69–80.
[44] J.M. Van der Laan, A.M., Riemens, W.J. Quax, US patent 5891703A, 1999 Apr 6.
[45] R.S. Topgi, J.S. Ng, B. Landis, P. Wang, J.R. Behling, Bioorg. Med. Chem. 7 (1999) 2221–2229.
[46] V.A. Soloshonok, N.A. Fokina, A.V. Rybakova, I.P. Shishkina, S.V. Galushko, A.E. Sorochinsky, V.P. Kukhar, M.V. Savchenko, V.K. Švedas, Tetrahedron Asymmetr. 6 (1995) 1601–1610.
[47] J.H. Cohen, M.E. Bos, S. Cesco-Cancian, B.D. Harris, J.T. Fortenstine, M. Justus, C.A. Maryanoff, J. Mills, S. Muller, A. Roessler, L. Scott, K.L. Sorgi, F.J. Villani, R.R.H. Webster, C.h. Weh, Org. Proc. Res. Dev. 7 (2003) 866–872.
[48] L.G. Frederick, O.D. Suleymanov, J.A. Szalony, B.B. Taite, A.K. Salyers, L.W. King, L.P. Feigen, N.S. Nicholson, Circulation 25 (1998) 813–820.
[49] J. Rudat, B.R. Brucher, C. Syldatk, AMB Express 2 (2012) 11–21.
[50] J. Hu, Y.C. Xue, M.Y. Xie, R. Zhang, T. Otani, Y. Minami, Y. Yamada, T. Tarunaka, J. Antibiot. 41 (1988) 1575–1579.
[51] X. Gong, E. Su, P. Wang, D. Wei, Tetrahedron Lett. 52 (2011) 5398–5402.